1999

Computation of Flame Base Height of a Turbulent Diffusion Flame Resulting From a Methane Jet

A. S. Kheireddine
Old Dominion University

S. K. Chaturvedi
Old Dominion University

T. O. Mohieldin
Old Dominion University

Original Publication Citation

Kheireddine, A. S., Chaturvedi, S. K., & Mohieldin, T. O. (1999). Computation of flame base height of a turbulent diffusion flame resulting from a methane jet. *JSME International Journal Series B Fluids and Thermal Engineering*, *42*(1), 78-90. doi:10.1299/jsmeb.42.78

Computation of Flame Base Height of a Turbulent Diffusion Flame Resulting from a Methane Jet*

A. S. KHEIREDDINE**, S. K. CHATURVEDI**
and T. O. MOHIELDIN***

This work summarizes numerical results for a diffusion flame formed from a cylindrical tube fuel injector, issuing a gaseous methane jet vertically in a quiescent atmosphere. The primary objective is to predict the flame base height and other flame characteristics as a function of the fuel jet velocity. A finite volume scheme is used to discretize the time-averaged Navier-Stokes equations for the reacting flow resulting from the turbulent fuel jet motion. The turbulent stresses, and heat and mass fluxes are computed from a Reynolds stress turbulence model. A chemical kinetics model involving two-step chemistry is employed for the oxidation of methane. The reaction rate is determined from a procedure which computes at each point the minimum (process limiting) rate from an Arrhenius (kinetically controlled) expression and the eddy dissipation (turbulent mixing controlled) model. The Reynolds stress model (RSM), in conjunction with the two-step kinetics and the eddy dissipation model, produces flame base height and other flame characteristics that are in good agreement with experimental results. Numerical results are also in agreement with the hypothesis of Van Quickenbourn and van Tiggelen concerning the stabilization mechanism of lifted diffusion flames. The present results show the existence of the condition of tangency, as postulated by Van Quickenbourn and Van Tiggelen, between the jet axial velocity and the flame velocity profiles at the flame base. Furthermore, the burnout rate calculations indicate a high degree of premixing of air and fuel upstream of flame base for moderate to high fuel jet velocity cases.

Key Words: Turbulent Diffusion Flame, Lift-Off Height, Flame Stabilization Mechanism, Cylindrical Injector, Burnout Rate, Eddy Dissipation Model, Finite Rate Chemistry

1. Introduction

Diffusion flames have been studied extensively due to wide ranging applications in industrial and residential gas furnaces and jet engine combustors. Characteristics such as flame length and width have been measured and analyzed by many previous researchers. In recent years, considerable research efforts have directed towards developing theories to analyze the lift-off phenomenon in diffusion flames. Prediction of flame base height is important in design of combustors, and in determination of thermal loads on flame holders and other combustor surfaces. A review of various models for prediction of flame lift-off phenomenon in diffusion flames has been given by Pitts[1]. Two distinct approaches have been pursued to explain the observed flame lift-off phenomenon. The classical approach, due to Van Quickenbourn and van Tiggelen[2], assumes the existence of a premixed fuel-air mixture zone near the flame base. The propagation of flame, with the turbulent flame speed, into the oncoming flow results in a stably lifted flame at a

* Received 24th December, 1996
** Department of Mechanical Engineering, Old Dominion University, Norfolk, Virginia, 23529, USA. E-mail: skc@mem.odu.edu
*** Department of Engineering Technology, Old Dominion University, Norfolk, Virginia, 23529, USA

location where the flame speed equals the local velocity. Other studies subscribing to the premixed flame base concept include the works of Annushkin and Sverdlov[3], Hall et al.[4], Günther et al.[5] and Kalaghatgi[6].

The concept of pre-mixed flame base has been challenged by others who contend that it is unlikely that, based on characteristic diffusion length and time scales, sufficient mixing of fuel and air would occur at molecular level near the flame base. A recent development has been the emergence of the flamelet concept to predict the flame lift-off height in turbulent diffusion flames. Although several related ideas have been proposed, the central thesis is that the absence of flame near the fuel injector point is due to extinction of laminar flamelets. Prominent studies following this approach are due to Janicka and Peters[7], Peters and Williams[8], Peters[9], Bradley et al.[10] and Sanders and Lamers[11]. Peters and Williams[8] have used the scalar dissipation rate as the stretch parameter while Sanders and Lamers have used the strain rate of the smallest eddies as the parameter describing the flame stretch. Once the stretch parameter exceeds a critical value quenching of the flamelets occurs. These models generally involve additional empirical constants which do not have universal values and are determined by calibrating theoretical predictions against the observed results for the flame lift-off height. For example, Sanders and Lamers[11] report good agreement for flame base height with fuel exit velocity if the strain rate of the smallest eddies is used. However, the constant $C_{s,1}$ in their model does not have a universally accepted value. Values of $C_{s,1}=0.27$ for the flame lift-off case, and a value of $C_{s,1}=0.116$ for the isothermal case are suggested. In contrast Bradley et al.[10] use a value of $C_{s,1}=0.081$ in their mixedness-reactedness flamelet model. Sanders and Lamers also report uncertainty in numerical value of the critical strain rate used for the flamelet quenching criterion, and in the value of percolation threshold used in the criterion for locating the flame base. Despite these uncertainties, their results do point to the fact that strain rate of small eddies is the proper flame stretch parameter as compared to the scalar dissipation. Although many observed features of diffusion flames are adequately predicted by flamelet models, some discrepancies still remain. For example, Sanders and Lamers[11] report that the axial location where temperature begins to increase on the axis is about four times greater than in the study by Bradley et al.[10] It should be also noted that one of the basic premise of the flamelet models, e.g., no substantial mixing of fuel and air upstream of the flame base, has been questioned by many authors including Eickhoff et al.[12] and Sobiesiak and Brzustowski[13]. Experimental results reported by Pitts[1] also indicate substantial premixing in region upstream of the flame base. Pitts[14] has also shown that the lift-off height as a function of jet velocity can be predicted by consideration of the isothermal concentration and velocity profiles in the turbulent axisymmetric jet upstream of the flame base.

In the present study, the diffusion flame lift-off problem is addressed by using the eddy dissipation model for turbulent combustion. This model, first proposed by Magnussen and Hjertager[15], calculates the reaction rate in the mixing controlled combustion by determining the rate of mixing on a molecular scale in eddies containing fuel and oxidizer. This model is in some respect similar to the Spalding's eddy break-up model[16]. However, an important difference is that unlike the eddy break-up model it does not require prediction of fluctuation of reacting species. The eddy dissipation model (EDM) also takes into account the intermittency of concentration of reacting species by considering the dissipation of eddies containing different species that can be rate determining for different conditions. This feature is important in the present study since the base of the flame may lie in the region characterized by the intermittency of fuel and oxidizer concentration (Pitts[14]). The eddy dissipation model has been used by others, including Bai and Fuchs[17]. Although this model is heuristic in nature, and lacks the theoretical foundation of the flamelet models, it does offer a simple way of treating combustion in turbulent flows. In regions away from the injector point, its predictions, as reported by Magnussen and Hjertager[15], and Mohieldin and Chaturvedi[18], are in reasonable agreement with experimental results. The success of this model in predicting near field phenomenon such as the flame base height has not been documented in the literature. Although, some previous researchers, for example Bai and Fuchs[17], have reported the need to adjust constants in the eddy dissipation model to obtain results that are consistent with experimental results, the present study on the contrary establishes the fact that universal set of constants can be used in the EDM for variety of fuels and jet velocity conditions provided the Reynolds stress model is used for turbulence modeling instead of the k-ϵ model. In the present study, we have used the eddy dissipation model in conjunction with a Reynolds Stress Model (RSM) to predict the flame base lift-off distance of a methane-air turbulent diffusion flame. The effects of fuel jet velocity on the flame base height and other flame characteristics are examined for a circular tube fuel injector operating in a still environment.

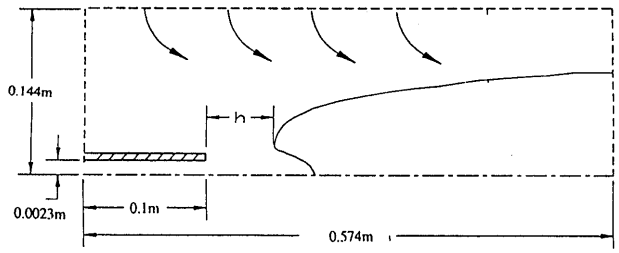

Fig. 1 Schematics of the lifted turbulent diffusion flame

Nomenclature

C_1, C_2, C_3, C_4, C_μ : constant in turbulent model
d : fuel jet diameter, m
g_i : gravitational accelerations, ms^{-2}
h : lift-off height, m
h_i : specific enthalpy of species i
k : turbulent kinetic energy
m_i : mass fraction of species i
R_i : reaction rate
r : radial direction, m
T : temperature, k
u : axial velocity, ms^{-1}
u_i : fluctuating component of velocity vector, ms^{-1}
x : axial direction, m
δ_{ij} : Kronecker delta
ϵ : turbulent kinetic energy dissipation
μ : molecular viscosity, $kgm^{-1}s^{-1}$
ρ : fluid density, kgm^{-3}
ν : kinematic viscosity, m^2s^{-1}
σ_n, σ_m, : turbulent Schmidt/prandtl numbers
ϕ : generalized scalar quantity

Subscripts
eff : effective
t : turbulent

2. Physical Model

The schematics of the physical system analyzed in the present study is shown in Fig. 1. A circular tube of 0.46 cm inside diameter, and 0.1 meter in length is used as the fuel injector. The tube has a wall thickness of 0.089 cm. Methane is the fuel used in the present study, and it is injected vertically in a quiescent atmosphere. The gas jet entrains the surrounding air, and the combustion ensues at a short distance form the bube opening. The flame base height (h), measured as the axial distance between the tube opening and the base of the flame (Fig. 1), depends on several parameters, namely the type of fuel, fuel jet velocity and the tube diameter. In order to assess the effects of these parameters numerically, a computational domain 0.29 meter in diameter and 0.58 meter in length was chosen.

Table 1 Conservation terms corresponding to Eq. (1)

Cons. of	ϕ	Γ_ϕ	S_ϕ
Mass	1	0	0
x-Momentum	u	μ	$-\frac{\partial p}{\partial x}+S_u$
r-Momentum	v	μ	$-\frac{\partial p}{\partial r}+S_v$
Energy	h	$\frac{k}{c_p}$	$\Sigma h_j R_j$
Mass Fraction	m_j	$\frac{\mu}{Sc}$	R_j

3. Governing Equations

The jet Reynolds number in the present study ranged from 6 000 to 15 000, indicating that flow is essentially turbulent[19]. The theoretical treatment of turbulent flows ranges from direct numerical simulation (DNS) to the solution of averaged Navier-Stokes equations. The former approach, due to prohibitively large computational requirements, is restricted to very simple geometries with small Reynolds number. In most practical geometries involving reactive flows, one uses either the density weighted (Favre) averaging or the density unweighted (Reynolds) averaging. In a recent paper, Soong et al.[20] have compared the numerical results obtained from the Reynolds and Favre averaging procedures for a turbulent diffusion flame in a coaxial sudden expansion combustor. Their results, although not conclusive, indicate that the Reynolds averaging procedure yields results closer to the observed results for the chosen geometry as compared to those obtained from the Favre averaging procedure.

In the present study, the Reynolds averaging procedure is adopted for obtaining the averaged gov erning equations for the transport of x-momentum, r-momentum, energy and species. These equations can be expressed in a general form as:

$$\frac{\partial}{\partial x}(\rho u\phi)+\frac{1}{r}(r\rho v\phi)=\frac{\partial}{\partial x}\left[\Gamma_\phi\frac{\partial\phi}{\partial x}-\overline{\rho u'\phi'}\right]+\frac{1}{r}\frac{\partial}{\partial r}\left[r\Gamma_\phi\frac{\partial\phi}{\partial r}-r\overline{\rho v'\phi'}\right]+S_\phi \quad (1)$$

The variable ϕ represents u, v, h and m_j, and expressions for Γ_ϕ and S_ϕ are given in Table 1. The turbulent stress terms $-\overline{\rho u'u'}$, $-\overline{\rho u'v'}$ and $-\overline{\rho v'v'}$ are predicted by employing a Reynolds Stress Model (RSM), described by Launder and Spalding[21]. The governing equation for $\overline{u_i'u_j'}$ can be expressed as

$$u_k\frac{\partial}{\partial x_k}(\overline{u_i'u_j'})=\frac{\partial}{\partial x_k}\left[\frac{\gamma t}{\sigma_h}\frac{\partial}{\partial x_k}(\overline{u_i'u_j'})\right]+P_{ij}$$

$$-C_3\frac{\epsilon}{k}\left(\overline{u_i'u_j'}-\frac{2}{3}\delta_{ij}\right)-C_4\left(P_{ij}-\frac{2}{3}\delta_{ij}P\right)$$
$$-\frac{2}{3}\delta_{ij}\epsilon \quad (2)$$

where P_{ij} can be expressed as

$$P_{ij}=\overline{u_i'u_k'}\frac{\partial u_j}{\partial x_k}+\overline{u_j'u_k'}\frac{\partial u_i}{\partial x_k} \quad (3)$$

The turbulent viscosity μ_t is given by the following expression

$$\mu_t=\rho C_\mu\frac{k^2}{\epsilon}\ ;\ k=\Sigma\frac{1}{2}\overline{u_i'u_i'}$$

The governing equation for dissipation (ϵ) can be expressed as

$$\frac{\partial}{\partial x}(\rho u\epsilon)+\frac{1}{r}(r\rho v\epsilon)=\frac{\partial}{\partial x}\left(\frac{\mu_{eff}}{\sigma_\epsilon}\frac{\partial\epsilon}{\partial x}\right)$$
$$+\frac{1}{r}\frac{\partial}{\partial r}\left(r\frac{\mu_{eff}}{\sigma_\epsilon}\frac{\partial\epsilon}{\partial r}\right)+\frac{\epsilon}{K}(C_1S_\epsilon-C_2\rho\epsilon) \quad (4)$$

where

$$S_\epsilon\equiv\mu_{eff}\left[\partial\left(\frac{\partial u}{\partial x}\right)^2+2\left(\frac{\partial v}{\partial r}\right)^2+2\frac{v^2}{r}+\left(\frac{\partial u}{\partial r}+\frac{\partial v}{\partial x}\right)^2\right]$$

and,

$$\mu_{eff}=\mu_t+\mu$$

In the present version of RSM, the turbulent fluxes for enthalpy and species are not obtained from separate transport equations. Instead, gradient hypothesis is used, along with appropriate turbulent Prandtl numbers to express turbulent fluxes in terms of appropriate gradients of properties.

$$-\overline{\rho u_i'h'}=\frac{\mu_t}{\sigma_h}\frac{\partial\phi}{\partial x_i} \quad (5)$$

and

$$-\overline{\rho u_i'm_i}=\frac{\mu_t}{\sigma_m}\frac{\partial m_i}{\partial x_i} \quad (6)$$

The turbulent Schmidt and Prandtl numbers (σ_m and σ_h) are taken as 0.7. Various constants, used in the Reynolds stress model identical to those reported by Launder and Spalding[21]. No attempt was made in this study to modify the universally accepted set of constants used in the Reynolds stress model.

The set of Eqs.(1)-(6) describe mathematically the turbulent combustion problem considered here. The combustion model discussed in a subsequent section determines the source and sink terms, S_ϕ, in Eq.(1). Equations (1)-(6) are solved numerically subject to specified boundary conditions.

4. Boundary Conditions

The constant pressure boundary condition was applied on the open boundaries. On the solid surface, the no slip condition was applied. On the fuel side, a known inlet axial velocity profile, obtained from a separate calculation of the flow field inside the tube, was used. Turbulent intensity of 9% was used at the fuel inlet section. Calculations with the inlet turbulence intensity of 15% showed that increasing the intensity results in thinning of the flame base due to reduced base width. However, the effect of turbulence intensity on the flame base height was negligible. Consequently, all calculations were performed with 9% inlet turbulence intensity. The inlet fuel temperature of 305 K was used so that results can be compared with the experimental results obtained at the same inlet temperature. The k and ϵ values at inlet were obtained from the specified values of turbulence intensity and the characteristic length scale of the tube. For the RSM, the inlet values of Reynolds stresses were also calculated from the specified turbulence intensity or the k-value.

5. Combustion Model

The chemical reactions rates are determined from a combination of the eddy dissipation model and a two-step chemical kinetics model. The eddy dissipation model relates the mixing controlled reaction rate to the mean concentration of species and a characteristic time (k/ϵ) for the dissipation of smallest turbulent eddies to molecular levels where chemical reaction takes place. In this model the rate of reaction is given by the smallest of the three expressions given below

$$(\dot{R}_{j,k})_{mixing}=\min\left[A\bar{\rho}\frac{\epsilon}{k}m_{fuel}\ ;\ A\bar{\rho}\frac{\epsilon}{k}m_{oxygen}\ ;\right.$$
$$\left.\nu_{j,k}M_jAB\bar{\rho}\frac{\epsilon}{k}\frac{\sum m_p}{\sum\nu_{p,k}M_p}\right] \quad (7)$$

where $\nu_{j,k}$ is the molar stoichiometric coefficient for species j in reaction k, A and B are empirical constants equal to 4 and 0.5 respectively, as recommended by Magnussen and Hjartager[15]. Subscript p denotes products, and M is the molecular weight of each species.

In regions where kinetics effects may be important, the reaction mechanism is approximated by a two-step kinetics model. The first step oxidizes methane to CO while the second step converts it to CO_2. As expected the two-step model produces higher flame base heights as compared to the single-step global reaction model. This is primarily due to the fact that the formation of CO is the rate limiting reaction which results in a slower temperature rise.

Table 2 Two-step model for methane/air reaction

Constant	R_{CH_4}	R_{CO}
k	1	2
A_k	5.28×10^{15}	1.60×10^{10}
E_k	2.2403×10^{8}	1.03716×10^{8}
α_k	0.5	1.0
β_k	1.0	1.0

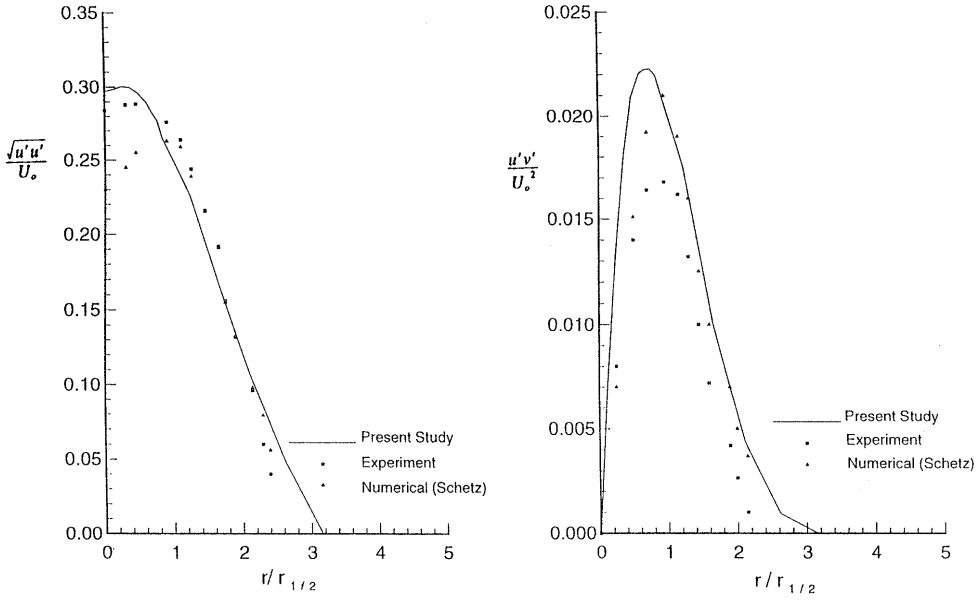

Fig. 2 Prediction of Reynolds stresses at axial location of 0.37 m. Experiment results from (Wygnanski & Fieldler)

The reaction rates for both steps are given in Eqs. (8) and (9).

$$CH_4+\frac{3}{2}O_2 \rightarrow CO+2H_2O\ ;\ (R_{CH_4}) = -M_{CH_4}A_1C_{CH_4}^{\alpha_1}C_{O_2}^{\beta_1}e^{-\frac{E_1}{RT}} \quad (8)$$

$$CO+\frac{1}{2}O_2 \rightarrow CO_2\ ;\ (R_{CO}) = -M_{CO}A_1C_{CO}^{\alpha_2}C_{O_2}^{\beta_2}e^{-\frac{E_2}{RT}} \quad (9)$$

The constants A_1, α_1, α_2, β_1, β_2, E_1 and E_2 are given in Table 2.

The source terms in the energy and mass transport equations depend on the reaction rate which in turn depends on whether the reaction is kinetically or diffusion controlled. In the combustion model used here, the reaction rates at any point in the flow field are calculated from the Arrhenius expressions (Eqs. (8)-(9)) and the eddy dissipation model (Eq. (7)). The lowest of these rates determines the process limiting rate. The constants in the eddy dissipation model and the Arrhenius model are taken respectively from Magnussen and Hjartager[15] and Westbrook and Dryer[22]. No attempt was made in this study to vary these universally accepted constants to obtain better agreement with experimental results.

6. Computational Procedure

In the present study a general purpose CFD code, known as "FLUENT", was used to obtain the flame lift-off characteristics. The "FLUENT" code[23] uses a finite volume method to discretize the governing transport equations into algebraic equations. The quadratic interpolation (QUICK) scheme has been used to discretize convective and diffusion terms in the transport equations[24]. The coupled algebraic equation for flow, temperature and concentration variables are solved by a semi-implicit method known as the "SIMPLE" technique[25].

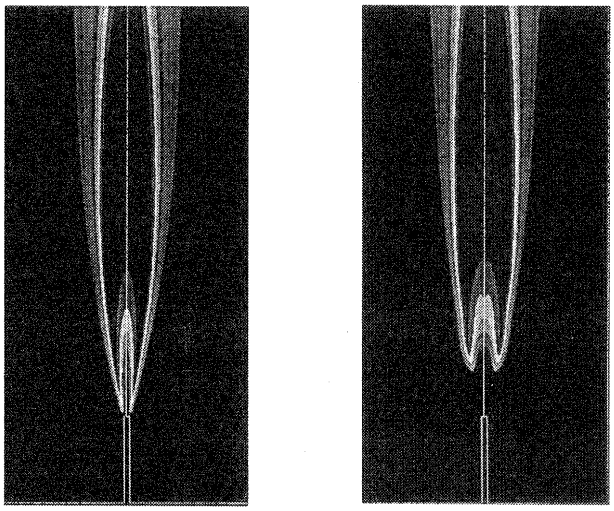

(a) (b)

Fig. 3 Flame structure for jet exit velocity of 34.7 m/s predicted by (a) k-ϵ model (b) RSM Model

Calculations were performed for both reacting and non-reacting flows by utilizing the (k-ϵ) model and the RSM. It should be noted that the RSM could not be executed directly without first implementing the k-ϵ model due to divergence of the calculation procedure. Two approaches have been used successfully to obtain the reacting flow solution with the RSM. In the first approach, the cold flow k-ϵ simulation is used as the initial field to obtain the cold flow

results with the RSM. Subsequently, with the combustion model included, the reacting flow results are obtained with the RSM. Alternatively, one can also directly employ the reacting flow solution from the k-ϵ model as the starting point to compute the reacting flow solution with the RSM.

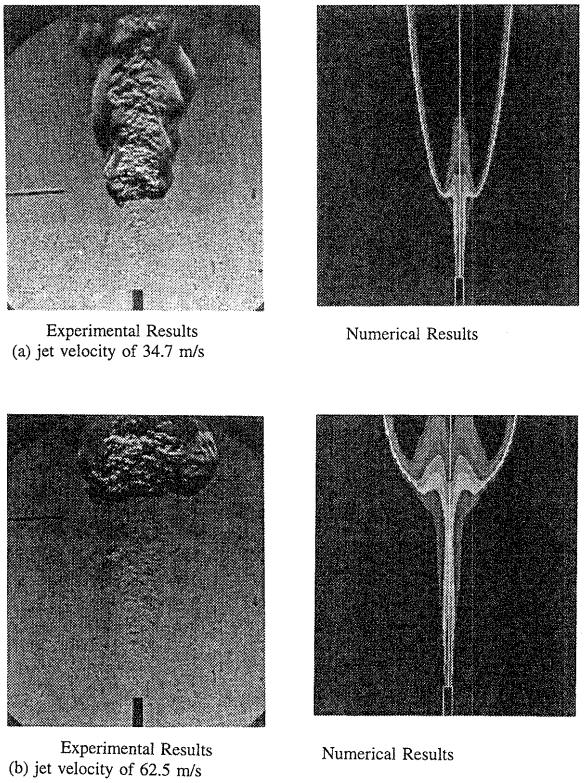

Experimental Results
(a) jet velocity of 34.7 m/s

Numerical Results

Experimental Results
(b) jet velocity of 62.5 m/s

Numerical Results

Fig. 4 Flame shape predicted from the present model as compared to experimental observations by Comer et al.

For all properties except pressure, the convergence was assumed to be achieved when residuals were less than 10^{-5}. For the pressure variable convergence was assumed when its residual was less than 10^{-4}. Prior to obtaining final results, three grids with number of nodes ranging from (70×41) to (140×81) were used. After detailed numerical experimentation for grid independence, the (151×61) grid was used for detailed results since it yielded grid independent results for both non-reacting as well reacting cases.

7. Numerical Results for Reacting Flows

Before undertaking detailed combustion calculations, results predicted from the RSM were validated for the non-reacting case by comparing them with results reported in literature for an air jet issuing from a circular tube[26]. The numerically predicted radial distributions of $\overline{u'u'}$ and $\overline{u'v'}$ in Fig. 2 compare very favorably with results reported by Schetz.

Combustion calculations were first performed with the k-ϵ model. Figure 3 shows the comparison of flames obtained from the (k-ϵ) and the Reynolds stress models in conjunction with the two-step kinetics and the eddy dissipation model. It is noted that the k-ϵ model produces a flame in which the flame base height is grossly underestimated compared to experiments. In contrast, the RSM produces flame whose base lift-off height is in good agreement with experimental results of Chen and Goss[27], Kalaghatgi[6] and Comer et al.[28] As a result, all

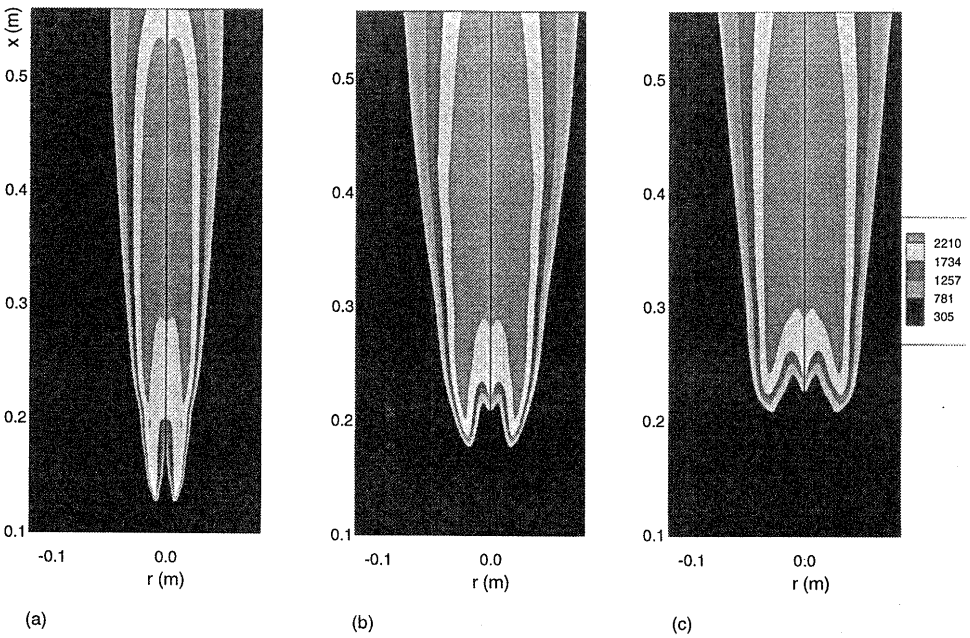

Fig. 5 Prediction of temperature field for flames at exit jet velocities of (a) 19 m/s, (b) 47.5 m/s and (c) 62.5 m/s

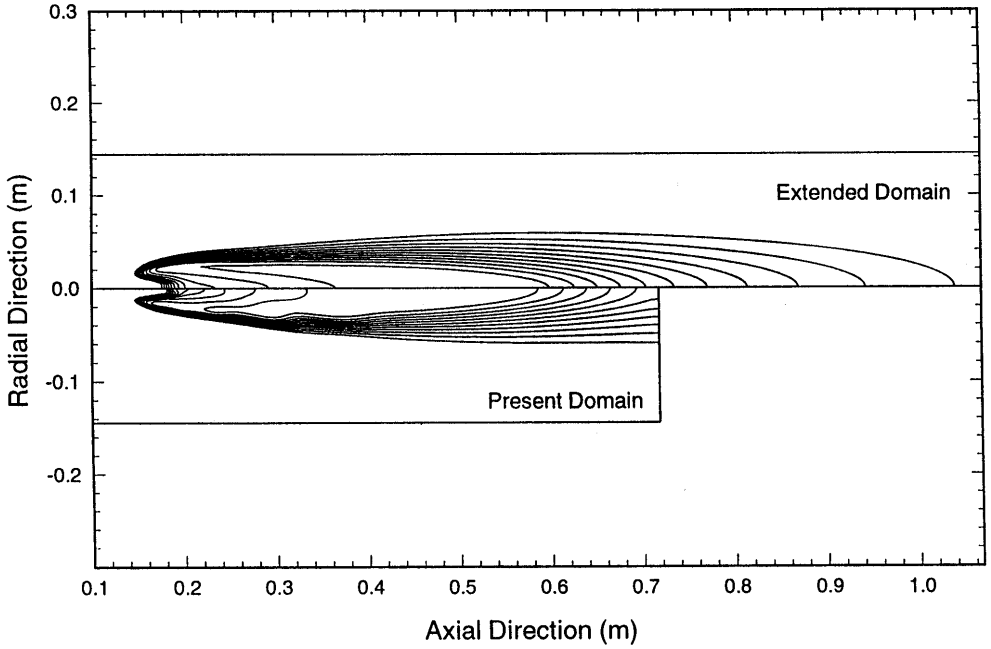

Fig. 6 Effect of extended domain length on the flame lift-off and structure predicted by (RSM) model for a fuel jet exit velocity of 34.7 m/s

numerical results presented in this study were obtained using the Reynolds stress turbulence model in conjunction with a two-step chemical kinetics model, and the eddy dissipation model. Results from the present numerical procedure were compared with experimental results reported by Comer et al.[28] who measured the flame base height for methane fuel jet by varying the fuel jet velocity. For numerical results, the tube diameter, length and wall thickness identical to those employed by Comer et al. were used.

Figure 4 shows the comparison of numerically obtained flame shape with the Schlieren photographs of the flame[28] for jet velocities of 34.7 m/s and 62.5 m/sec. Both numerical and experimental results for the 34.7 m/s case show a premixed region prior to establishment of the flame at a distance downstream of the injection point. The flame shape, base width, maximum width and base height obtained from computation compared favorably with experimental results. For the jet velocity of 62.5 m/s, the widening of flame base, and increase in flame base height are evident from both numerical and experimental results.

Figure 5 shows results obtained in the present study for fuel jet velocity ranging from 19 m/s to 62.5 m/s. Some general observations can be made concerning the numerical flame structure. The first one relates to the fact that for all jet velocities the flame is clearly lifted from the injection port. Also, the flame base height increases as the fuel jet velocity is increased. One visible effect is that the flame, as expected, becomes wider and longer in height and the flame base width increases with the increasing fuel jet velocity. It is noted that in every flame except the one for 62.5 m/s case there is a conical core region centered around the axis where the unreacted fuel penetrates into the interior region of the flame. This region is characterized by high methane and low oxygen concentrations, and low temperatures. The unreacted fuel jet penetration depth relative to the flame base height decreases with increasing jet velocity, thus resulting in the flame base flattening shown for the highest velocity case in Fig. 5. In fact, for this case the numerical flame exhibits a double dip. The flame front advances upstream in the axial region, forming a local flame base, in addition to the flame base at an off-axis location. This flame base broadening, also evident in the Schlieren photographs (Fig. 4) taken from the study be Comer et al.[28] is indicative of premixing in the region upstream of the flame base. All flames shown in Fig. 5 extend in axial direction beyond the chosen numerical domain. In order to resolve the question of the truncated computational domain affecting the flame base height calculations, a longer axial domain of about one meter length was chosen in Fig. 6 for the 34.7 m/s jet velocity case. This calculation produced a full flame in the computational domain. The flame base height calculated from the larger domain differed from the one for the truncated flame in the smaller domain in Fig. 5 by less than 0.5%. This validated the present approach of reducing the computational effort by using smaller computational domain to calculate the flame base

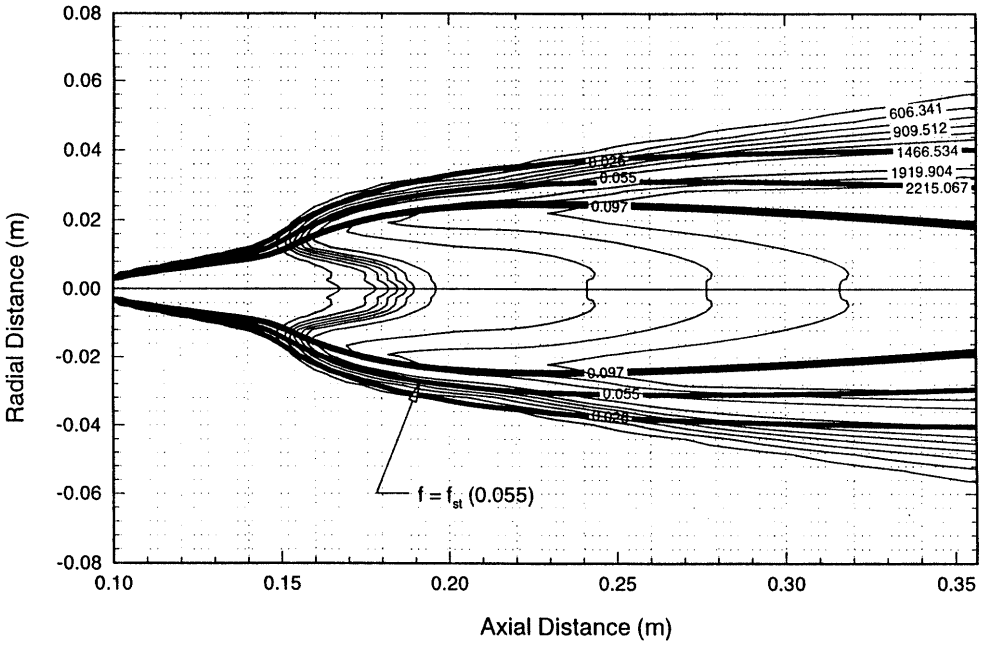

Fig. 7 Expanded view of temperature and mixture fraction (f) contours for the fuel jet exit velocity of 34.7 m/s

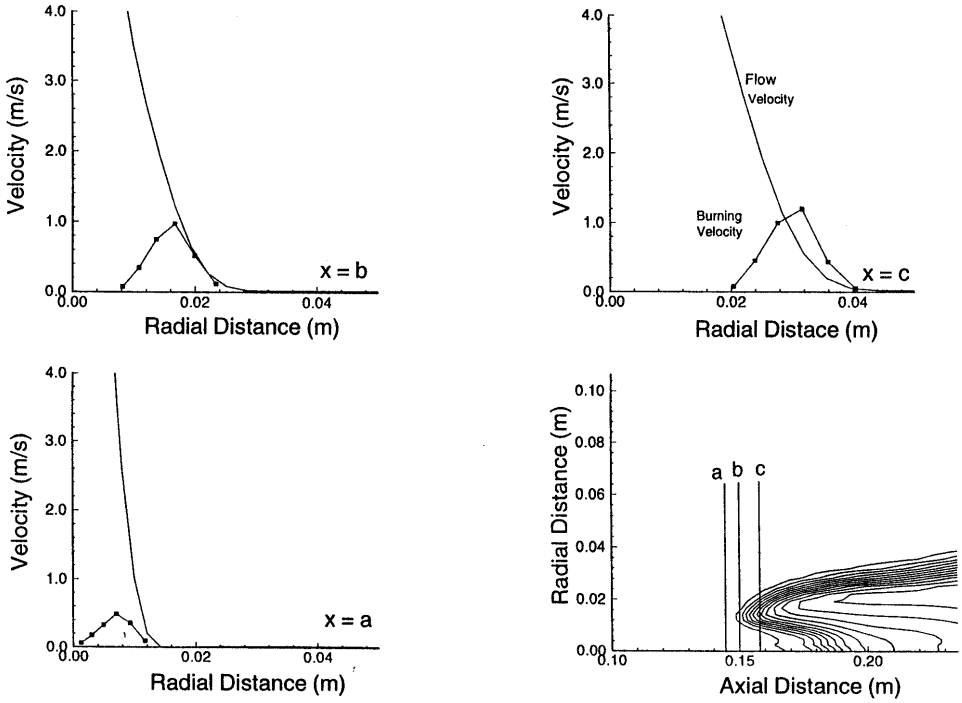

Fig. 8 Velocity profiles at different axial locations (a=.042 m, b=.051 m, c=.06 m) for a fuel jet exit velocity of 34.7 m/s — flow velocity, —■—turbulent burning velocity

height.

Figure 7 shows an expanded view of temperature contours near the flame base. Also superimposed on this figure are the numerically obtained contours for mixture fraction. The 0.097, 0.055 and 0.026 contours represent for methane the upper flammability (rich) limit, the stoichiometric case and the lower flammability (lean) limit respectively. One observes that the potentially flammable region, based on the stability criterion, expands from a narrow width at the injection point to a larger width near the flame base. In this regard, one should also note a remarkable similarity between this figure and the one given by Van Quickenbourn and van Tiggelen[2] who postulated

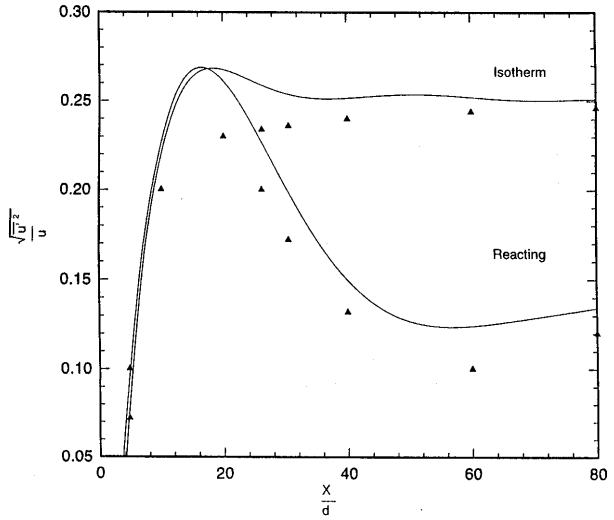

Fig. 9 Axial values of calculated turbulent intensity (solid lines) as compared with experimental measurements (symbols) for reacting and non-reacting cases

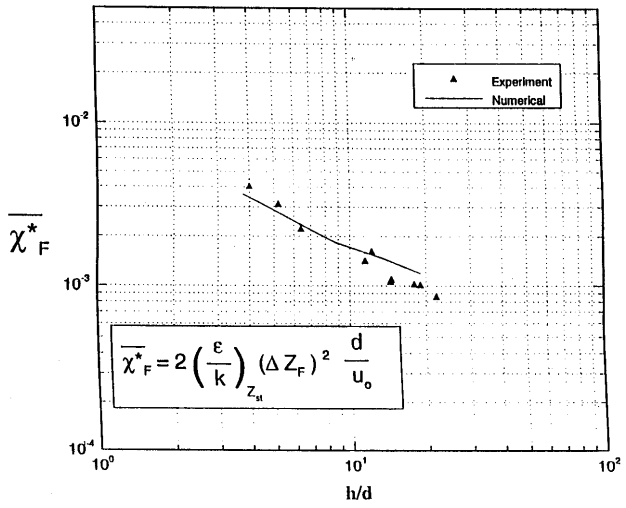

Fig. 10 Comparison of predicted non-dimensional scalar dissipation with experimental data for lifted methane flames

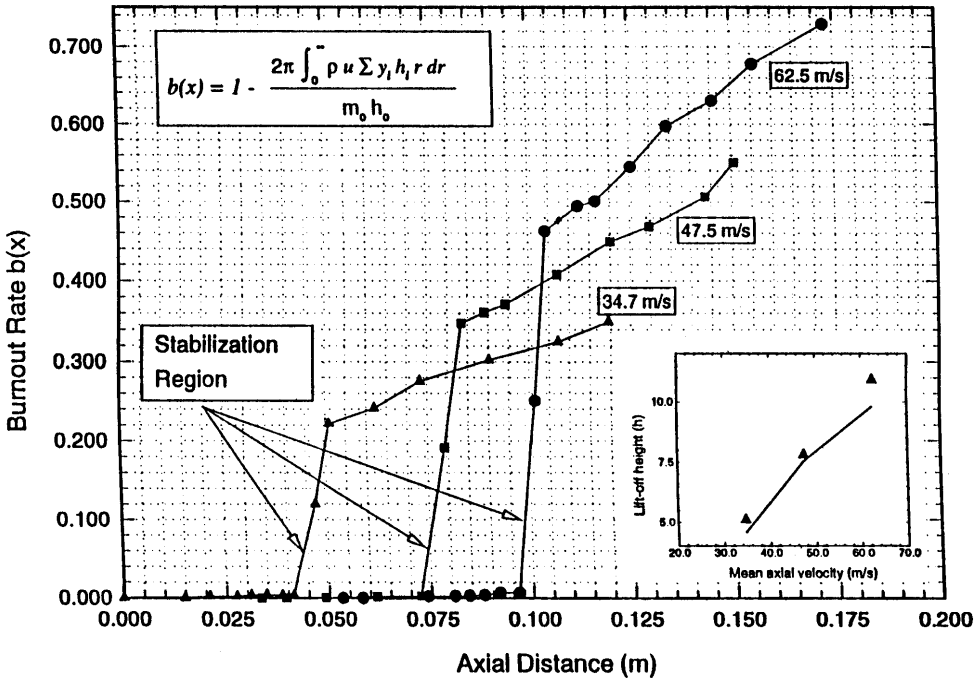

Fig. 11 Prediction of burnout rate along axial direction for jet exit velocity of 34.7 m/s 47.5, and 62.5 m/s. Small graph represents lift-off height predicted using turbulent flame speed criterion (symbols) as compared to the burnout rate criterion (lines)

anchoring of the lifted diffusion flame in a premixed region. From Fig. 7, it is clear that the numerical flame is stabilized in the flammable region, in the proximity of the stoichiometric methane concentration contour.

Figure 8 shows the radial variation of axial component of velocity and the turbulent flame velocity, computed from a procedure described by Kalaghatgi[6] for the 34.7 m/s jet velocity case. Three axial locations namely $x=0.042$ m (upstream of the flame base) $x=0.051$ (flame base) and $x=0.06$ m (downstream) are considered. For upstream locatons it is apparent that the flame velocity is lower than the flow velocity at all radial locations. The profiles at the flame base exhibit the tangency condition while profiles at downstream locations show that the flame velocity is

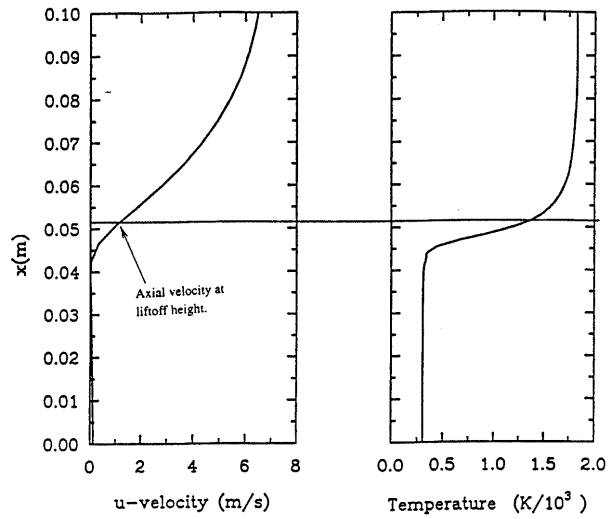

Fig. 12 Variation of u-component and temperature along axial traverse at radial location of 0.0165 m

greater than the flow velocity at several radial locations. These computed results are remarkably similar to those described by Van Quickenbourn and van Tiggelen in their classical paper dealing with flame stabilization phenomenon. Similar behavior is also observed for numerical results for other fuel jet velocities. At the point of tangency, characterizing the flame stabilization point, the turbulent flame velocity equals the flow velocity. This condition has been used in the present study to determine the location of the flame base. Since most experimental studies indicate that the flame stabilizes on the stoichiometric line, this fact has been used in the numerical calculations to locate the radial position of the flow base.

Figure 9 shows the comparison of the numerically predicted values of $\sqrt{\overline{u'u'}}/\bar{u}$ for reacting case with the experimental observations of Eickhoff et al.[12] The agreement between the experiments and numerical calculations is reasonably good except for the peak value of $\sqrt{\overline{u'u'}}/\bar{u}$ which is somewhat overpredicted in the numerical case. Also, the axial location of the peak value point is somewhat underestimated in the numerical calculations. Figure 10 shows the comparison of numerically predicted non-dimensional scalar dissipation from the present study with the experimental data of the lifted methane flame[29]. It can be seen that the present numerical scheme yields results that are in very good agreement with experimentally measured scalar dissipation.

Figure 11 shows results from a different method that uses the fuel burnout rate as the criterion for predicting the flame stabilization region (Eickhoff et al.[12]). The rate of burnout $b(x)$ at a given axial location is determined by integration of mass weighted enthalpy fluxes at that section. Eickhoff et al. have

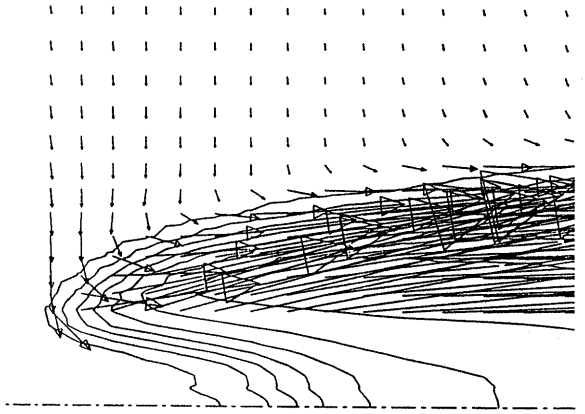

Fig. 13 Magnified view of velocity vectors and temperature field at the flame base

argued that the burnout rate is indicative of the premixing that takes place prior to the flame base. The numerically calculated burnout rate is shown in Fig. 11 for three jet velocities. The results show same trends as the experimentally observed values of $b(x)$ reported in Ref.(12). For instance, for the 47.5 m/s case the burnout rate is nearly zero upstream of a given axial location and it rises steeply to a value of about 0.35 in a very short axial distance. The slope of the $b(x)$ curve changes abruptly at a point slightly down stream of the flame stabilization region. This can be explained by the fact that the substantial premixing of air and fuel upstream of the flame base results in rapid combustion that sustains a higher burn out rate in the vicinity of the flame base. However, the mixing of ambient air due to entrainment drops abruptly downstream of the flame stabilization region, and this results in a lower reaction rate and a smaller slope for the burnout rate. For the 62.5 m/s jet velocity case, the slope of the $b(x)$ curve is higher, and it reaches a higher burnout rate value of about 0.46 before the abrupt change in slope occurs. Conversely, the 34.7 m/s jet velocity case produces a smaller slope for the $b(x)$ curve and a value of $b(x)=0.22$ at the point where the slope change occurs.

These results reaffirm the validity of models of many previous researchers[2)-6),29] who have postulated premixing to explain the flame stabilization phenomenon. Present results indicate that at moderate to high fuel jet velocities sufficient premixing of air and fuel occurs prior to the flame base to justify use of premixed flame models.

Figure 12 shows the variation of the u-component of velocity and temperature along an axial traverse at a radial location of $r=0.0165$ m, a location coincident with the flame base stabilization point for the 34.7 m/s jet velocity case. The temperature remains relatively constant in the region upstream of the flame base,

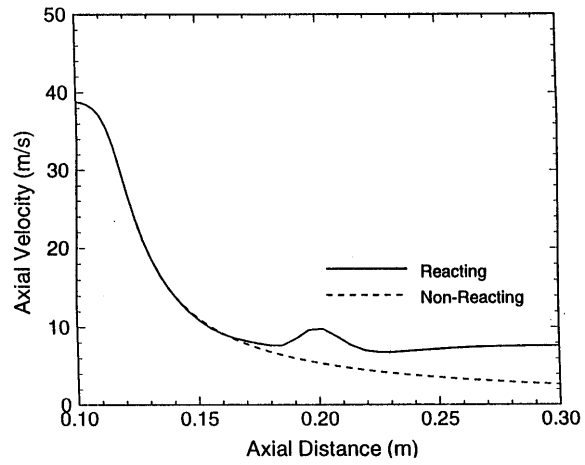

Fig. 14 Computed axial velocity for reacting and non-reacting flows

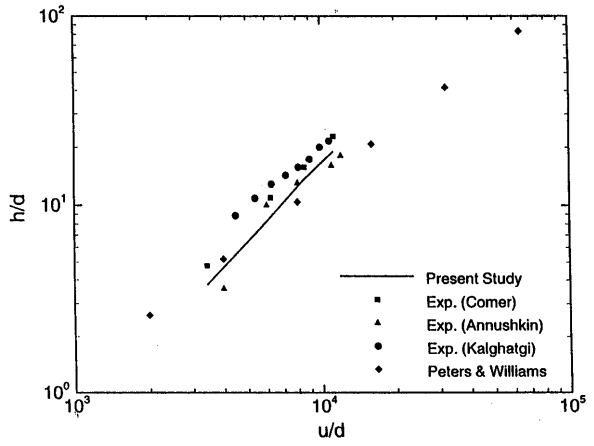

Fig. 15 Variation of flame base height to tube diameter ratio with fuel jet velocity to diameter ratio

and then rises steeply as the flame base is approached. The u-velocity component first shows a steady decline along the x-direction, reaches a zero value and then increases sharply due to the heat release that causes a sharp drop in density. This feature has been described by Bradley et al.[10] as the thermal expansion zone. This is further illustrated in Fig. 13 which shows the velocity vector field superimposed on the temperature field of the flame. The fuel jet entrains surrounding air which sustains combustion in the flame. It is also noted that ambient air at off-axis locations shows a velocity field in which the u-component of velocity is quite small. However, in the premixed region near the flame base, due to thermal expansion, the u-component of velocity vector becomes quite large, and shows a sharp rise along the x-direction. Figure 14 shows the variation of axial velocity for the reacting and non-reacting cases. The non-reacting case shows a sustained decay with the axial distance while the reacting case shows a bump in the axial velocity in the combustion zone. Similar behavior has also been reported by Sanders and Lamers in their numerical procedure. However, as indicated in their paper, no corresponding experimental observation has yet been reported in the literature.

Figure 15 shows the variation of the flame base height to tube diameter ratio with jet velocity to diameter ratio. Results from the present study are compared with other existing numerical as well as experimental results. This figure clearly indicates that experimental results of various previous studies do not agree quantitatively with one another. For example, results reported by Annushkin and Sverdlov are much lower compared to those reported by Kalaghatgi. We note that present numerical results are in reasonable agreement with experimental results reported by Comer et al.[28] As noted earlier, and seen from Fig. 15, it is evident that the k-ϵ model grossly underestimates the flame base height. Although results underestimate experimental results of Kalaghatgi at low u/d values a better accord with experimental results is achieved at larger values of u/d. Current numerical results also reveal a linear relationship between the flame base height and the fuel jet velocity. The numerical results of Peters and Williams[8], using laminar flamelet theory, generally underpredict the experimental results of Kalaghatgi. The slope of the flame base height versus jet velocity curve, reported by Rokke et al.[30] using the Peters and Williams model[8], has a value of 1.3×10^{-3} as compared to a value of 1.45×10^{-3} obtained in the present study.

8. Conclusions

The Reynolds stress model was used in conjunction with a two-step chemical kinetics model and the eddy dissipation model to predict the flame base height of a diffusion flame formed by a turbulent fuel jet issuing in a quiescent atmosphere. The RSM predicts flame base heights that are in reasonable agreement with the experimentally observed flame base height results. The model also successfully predicts the linear relationship between the flames base height and the fuel jet velocity. The flame base widens and flattens as the fuel jet velocity is increased. At the highest jet velocity, the flame base shows a double dip pattern in which the flame front at the axis also advances to an upstream location. It is quite remarkable that the RSM has yielded reasonable results with universally accepted constants in turbulence and the chemistry models. In contrast, the (k-ϵ) model grossly underpredicts the flame base height when compared with experimental results. Numerical results using the RSM also reveal that the flame base, as postulated in a model by Van Quickenbourn and

van Tiggelen[2], is anchored in the pre-mixed flammable region on the stoichiometric line where u-component of flow velocity is in equilibrium with the local turbulent flame speed. Many other features of diffusion flames, as observed or predicted by others, have also been successfully calculated by the present model. These include the predicted bump in the axial velocity, the thermal expansion zone near the flame base and other flame characteristics such as the maximum width of the flame, and the flame height. The results also indicate that the position of the flame base is strongly governed by the turbulent mixing the fuel jet upstream of the flame base which results in substantial premixing of air and fuel ahead of the flame base. This is clearly indicated by the calculation of burnout rate at moderate to high jet velocity cases.

References

(1) Pitts, W., Assement of Theories for the Behavior and Blowout of Little Turbulent Diffusion Flames, Twenty-Second Symposium (International) on Combustion, (1988), p. 809.

(2) Van Quickenbourn, L. and van Tiggelen, A., The Stabilization Mechanism of Lifted Diffusion Flames, Combustion and Flame, Vol. 10 (1966), p. 59.

(3) Annushkin, Y. and Sverdlov, E., Stability of Submerged Diffusion Flames in Subsonic and Underexpanded Supersonic Gas-Fuel Streams, Combustion Explosion and Shock Waves, Vol. 14 (1979), p. 597.

(4) Hall, L., Horch, K. and Günther, R., Die Stabilator Von Fveistahl—Diffusions Flammer, Brennst-Warme-Kraft, Vol. 32 (1980), p. 26.

(5) Günther, R., Horch, K. and Lenze, B., The Stabilization Mechanism of Free Jet Diffusion Flame, First Specialists Meeting (International) of Combustion Institute, Bordeaux, (1981), p. 117.

(6) Kalaghatigi, G., Lift-Off Heights and Visible Lengths of Vertical Turbulent Jet Diffusion Flames in Still Air, Combustion Science and Technology, Vol. 41 (1984), p. 17.

(7) Janicka, J. and Peters, N., Prediction of Turbulent Jet Diffusion Flame Lift-Off Using a PDF Transport Equation, Nineteenth Symposium (International) on Combustion (1982), p. 367.

(8) Peters, N. and Williams, F., Lift-Off Characteristics of Turbulent Jet Diffusion Flame, AIAA Journal, Vol. 24 (1983), p. 423.

(9) Peters, N., Laminar Flamelet Concepts in Turbulent Combustion, Twenty-First Symposium (International) on Combustion, (1986), p. 1231.

(10) Bradley, P., Gaskell, H. and Lau, A., A Mixedness—Reactedness Flamelet Model for Turbulent Diffusion Flames, Twenty-Third Symposium (International) on Combustion, (1990), p. 685.

(11) Sanders, J. and Lamers, A., Modeling and Calculation of Turbulent Lifted Diffusion Flames, Combustion and Flames, Vol. 96 (1994), p. 22.

(12) Eickhoff, H., Lenze, B. and Leuckel, W., Experimental Investigation on the Stablization Mechanism of Jet Diffusion Flames, Twentieth Symposium (International) on Combustion, The Combustion Institute, (1984). p. 311.

(13) Sobiesiak, A. and Brzustowski, T., On the Structure of the Stabilization Region of Lifted Turbulent Diffusion Flames, 1986 Spring Meeting of the Western States Section of the Combustion Institute, Banff, Canada, April 27-30 (1986).

(14) Pitts, W., Importance of Isothermal Mixing Processes to Understanding of Lift-off and Blowout of Turbulent Jet Flames, Combustion and Flame, Vol. 76 (1989), p. 197.

(15) Magnussen, G. and Hjertager, B., On Mathematical Models of Turbulent Combustion with Special Emphasis on Soot Formation and Combustion, Sixteenth Symposium (International) on Combustion, (1976), p. 15.

(16) Spalding, D., Mathematical Models of Turbulent Flames: A Review, Combustion Science and Technology, Vol. 13 (1976), p. 3.

(17) Bai, X. and Fuchs, L., Sensitivity Study of Turbulent Reacting Flow Modeling in Gas Turbine Combustors, AIAA Journal, Vol. 33 (1995), p. 1857.

(18) Mohieldin, T. and Chaturvedi, S., Flame Lift-Off and Thermal Load Characteristics of a Cylindrical Injector, Numerical Methods in Thermal Problems, Vol. 8 (1993), p. 1346.

(19) Kanury, A., Introduction to Combustion Phenomena, (1992), Gordon and Breach, New York.

(20) Soong, H., Han, H. and Chang, K., Comparative Numerical Studies on Reynolds and Favre Averagings of Turbulent Diffusion Flame, Journal of Propulsion and Power, Vol. 8 (1992), p. 259.

(21) Launder, B. and Spalding, D., The Numerical Computation of Turbulent Flows, Imperial College of Science and Technology, (1974), NSIS N 74—12066.

(22) Westbrook, C. and Dryer, F., Simplified Reaction Mechanism for the Oxidation of Hydrocarbon Fuels in Flames, Combustion Science and Technology, Vol. 27 (1981), p. 31.

(23) Fluent Manual, (1993), V. 4.2, Fluent Inc., New Hampshire.

(24) Leonard, B., A Stable and Accurate Convective Modeling Procedure Based on Quadratic Upstream Interpolation, Computer Methods in Applied Mechanics and Engineering, Vol. 19 (1979), p. 59.

(25) Patankar, S. and Spalding, D., A Calculation Procedure for Heat Mass and Momentum Transfer in Three-Dimensional Parabolic Flows, Int. Journal of Heat Mass Transfer, Vol. 15 (1972), p. 1787.

(26) Schetz, J., Injection and Mixing in Turbulent Flow, Vol. 68 (1980), Progress in Astronautics

and Aeronautics.
(27) Chen, T. and Goss, L., Stabilization Zone Structure in Jet Diffusion Flames from Lift-Off to Blow-out, AIAA Paper 89-0153 (1989).
(28) Comer, K., Mohieldin, T., Tiwari, S. and Puster, R., Experimental and Numerical Investigations of Lifted Methane Diffusion Flames, AIAA Paper 95-0728 (1995).
(29) Bray, K. and Peters, N., Laminar Flamelet in Turbulent Flames, Turbulent Reacting Flows (1994), p. 63, Academic Press, Washington, D. C.
(30) Rokke, N., Hustad, J. and Sonju, O., A Study of Partially Premixed Unconfined Propane Flames, Combustion and Flames, Vol. 97 (1994), p. 88.